Asian Research Journal of Mathematics

7(4): 1-13, 2017; Article no.ARJOM.38424
ISSN: 2456-477X

Analysis of Heat Generating, Heat Conducting and Thermally Isolated Internal Solid Block Confined in a Ventilated Enclosure

M. U. Ahammad[1], M. H. Rashid[1*] and M. A. Rahman[1]

[1]Department of Mathematics, Dhaka University of Engineering and Technology (DUET), Gazipur-1707, Bangladesh.

Authors' contributions

This work was carried out in collaboration between all authors. Author MUA designed the study, performed the statistical analysis, wrote the protocol, and wrote the first draft of the manuscript. Authors MHR and MAR managed the analyses of the study. Author MHR managed the literature searches. All authors read and approved the final manuscript.

Article Information

DOI: 10.9734/ARJOM/2017/38424
Editor(s):
(1) Ruben Dario Ortiz Ortiz, Professor, Facultad de Ciencias Exactas y Naturales, Universidad de Cartagena, Colombia.
Reviewers:
(1) John Abraham, University of St. Thomas, USA.
(2) Ajaz Ahmad Dar, University of Kashmir, India.
Complete Peer review History: http://www.sciencedomain.org/review-history/22353

Original Research Article

Received 25th November 2017
Accepted 10th December 2017
Published 18th December 2017

Abstract

A numerical study is executed on laminar, incompressible viscous flow in a ventilated enclosure to clarify the flow and heat transfer characteristics of an electrically conducting fluid subjected to three different interior solid block. The Reynolds number, Prandtl number and Hartmann number are treated as governing parameters in this article. Galerkin-weighted residual based Finite Element method was applied for performing the solution of governing equations. In order to explore the effect of considered three obstacles along with studied parameters, detailed analysis were carried out for visualization of streamlines and isotherms that represents the flow pattern and temperature distribution inside cavity. In addition, average Nusselt number Nu_{av} at the bottom heated surface of the cavity is shown in tabular form. It is observed that maximum cooling effectiveness that is highest heat transfer rate is achieved for the case of heat conducting block for all considered parameters.

Keywords: Heat generating (HG); heat conducting (HC); thermally isolated (TI); solid block; ventilated enclosure.

**Corresponding author: E-mail: harun66@duet.ac.bd;*

1 Introduction

The knowledge of flow structure and heat transfer by combined forced and free convection in an enclosure is of interest in relation to a number of physical and technological applications such as ventilation, heat or pollution agent clearance, and electronic cooling. Several numerical and experimental studies have been done concerning the combined effect of the magnetic force and a solid obstacle on the convective flow and heat transfer inside enclosures. Whatever the type of the interior solid body, flow and heat transfer inside enclosures have numerous engineering applications, such as heat exchangers, energy storage, solar collectors, ovens, oven heat transfer, electric machinery, cooling systems for electronic devices, and natural circulation in the atmosphere. An improvement in cooling can be obtained when the heat conducting obstacle is placed in the center of the cavity.

Researchers have done many numerical works on heat and mass transfer; among these previous works Rahman et al. [1] investigated mixed convection in a vented square cavity with a heat conducting horizontal solid circular cylinder. Munshi et al. [2] discussed on modeling and simulation of MHD convective heat transfer of channel flow having a cavity. Prakash and Ravikumar [3] presented study of thermal comfort in a room with windows at adjacent walls along with additional vents. Ahammad et al. [4] performed effect of inlet and outlet position in a ventilated cavity with a heat generating square block. Rahman et al. [5] analyzed the effects of Reynolds and Prandtl number on mixed convection in a ventilated cavity with a heat-generating solid circular block. Loyola et al. [6] carried out natural convection through an open cavity heated from the side and filled with fluid and discrete solid blocks. Wanz et al. [7] discussed combined heat transfer by natural convection – conduction and surface radiation in an open cavity under constant heat flux heating. Ait-Taleb et al. [8] showed their research paper numerical simulation of coupled heat transfers by conduction, natural convection and radiation in hollow structures heated from below or above. Oztop et al. [9] carried out fluid flow due to combined convection in lid-driven enclosure having a circular body. Rahaman et al. [10] studied Reynolds and Prandtl numbers effects on MHD mixed convection in a lid-driven cavity along with joule heating and centered heat conducting circular block. Ahammad et al. [11] investigated mixed convection flow and heat transfer behavior inside a vented enclosure in the presence of heat generating obstacle. Gau et al. [12] presented an experimental study on mixed convection in a horizontal rectangular channel heated from a side. Kumar and Dalal [13] carried out a numerical study of natural convection around a square horizontal heated cylinder placed in an enclosure.

Obayedullah et al. [14] showed in their work natural convection in a rectangular cavity having internal energy sources and electrically conducting fluid with sinusoidal temperature at the bottom wall. Rahman et al. [15] presented in their work magnetohydrodynamic mixed convection in a horizontal channel with an open cavity. Xu Xu et al. [16] analyzed a numerical study of laminar natural convective heat transfer around a horizontal cylinder inside a concentric air-filled triangular enclosure. Habibis et al. [17] investigated natural convection in a differentially heated square enclosure with a solid polygon. Xu et al. [18] carried out transient natural convective heat transfer of a low-prandtl-number fluid from a heated horizontal circular cylinder to its coaxial triangular enclosure. Calmidi and Mahajan [19] studied mixed convection in a partially divided rectangular enclosure over a wide range of Reynolds and Grashof numbers. Their findings were that the average Nusselt number and the dimensionless surface temperature depended on the location and height of the divider. Bhoite et al. [20] studied numerically the problem of mixed convection flow and heat transfer in a shallow enclosure with a series of block-like heat generating component for a range of Reynolds and Grashof numbers and block-to-fluid thermal conductivity ratios. They showed that higher Reynolds number tends to create a recirculation region of increasing strength in the core region and the effect of buoyancy becomes insignificant beyond a Reynolds number of typically 600, and the thermal conductivity ratio had a negligible effect on the velocity fields.

Recently, Baranwal and Chhabra [21] showed effect of fluid yield stress on natural convection from horizontal cylinders in a square enclosure. Shateyi [22] observed heat and mass transfer for natural convection MHD flow over a permeable moving vertical plate with convective boundary condition in the presence of viscous dissipation. Altaee et al. [23] investigated natural convection inside square enclosure containing equilateral triangle with different orientations.

Ajaz and Elangovan [24] investigated the influence of thermal diffusion, radiation and inclined magnetic field on oscillatory flow in an asymmetric channel with heat source and chemical reaction. A simple model and validating experiments for predicting the heat transfer to a load situated in an electrically heated oven was performed by Abraham and Sparrow [25].

The overall aim of the current investigation is to explore steady laminar mixed convection flow and heat transfer characteristics in a ventilated square enclosure with three different types of solid body located at the center of the cavity and reveal a comparison of heat transfer rate among these studied obstacles.

2 Details of Studied Area

The physical domain of the considered problem is displayed in Fig. 1 that consists of a square enclosure of length L with three distinct solid blocks namely heat generating, heat conducting and thermally isolated one by one located at the center. All sides of the cavity were taken as thermally isolated whereas the bottom surface is kept at a constant temperature T_h. An external fluid flow enters the enclosure through an opening at bottom in the left vertical wall and exit from another fixed opening at top in the right vertical wall. The length of each port is one-tenth of cavity length that is $w = 0.1L$. Rigid no-slip walls is considered for all solid boundaries that is velocity components u and v are set to be zero. The flow enters into the cavity with a uniform velocity, u_i and ambient temperature, T_i whereas the departing flow is considered to have zero diffusion flux (outflow boundary conditions) for all dependent variables.

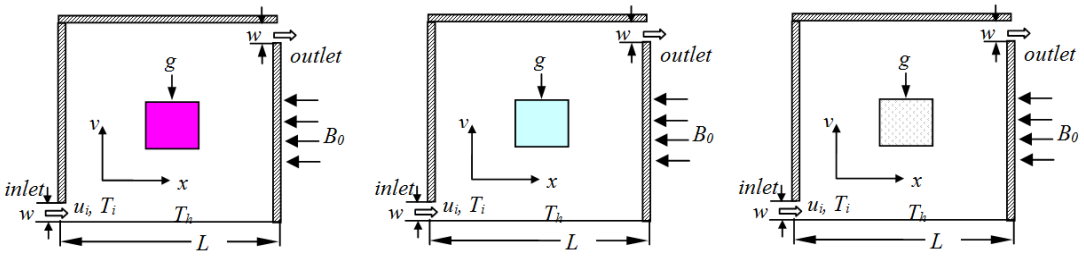

Fig. 1. The geometry under investigation

Free and forced convection is governed by the differential equations expressing conservation of mass, momentum and energy. The flow of the present problem is considered steady, laminar, incompressible and two-dimensional. The physical properties of the fluid in the flow model are assumed constant excluding the density variations body force term in the momentum equation. Moreover, the viscous dissipation term is neglected in the energy equation. The leading equations designed for steady state mixed convection flow can be expressed in the dimensionless form as

$$\frac{\partial U}{\partial X}+\frac{\partial V}{\partial Y}=0 \tag{1}$$

$$U\frac{\partial U}{\partial X}+V\frac{\partial U}{\partial Y}=-\frac{\partial P}{\partial X}+\frac{1}{\mathrm{Re}}\left(\frac{\partial^2 U}{\partial X^2}+\frac{\partial^2 U}{\partial Y^2}\right) \tag{2}$$

$$U\frac{\partial V}{\partial X}+V\frac{\partial V}{\partial Y}=-\frac{\partial P}{\partial Y}+\frac{1}{Re}\left(\frac{\partial^2 V}{\partial X^2}+\frac{\partial^2 V}{\partial Y^2}\right)+Ri\,\theta-\frac{Ha^2}{Re}V \tag{3}$$

$$U\frac{\partial\theta}{\partial X}+V\frac{\partial\theta}{\partial Y}=\frac{1}{\mathrm{Re}\,\mathrm{Pr}}\left(\frac{\partial^2\theta}{\partial X^2}+\frac{\partial^2\theta}{\partial Y^2}\right) \tag{4}$$

For heat generating solid block

$$\frac{K}{\mathrm{Re}\,\mathrm{Pr}}\left(\frac{\partial^2\theta_S}{\partial X^2}+\frac{\partial^2\theta_S}{\partial Y^2}\right)+Q=0 \tag{5}$$

For heat conducting solid block

$$\frac{K}{\mathrm{Re}\,\mathrm{Pr}}\left(\frac{\partial^2\theta_S}{\partial X^2}+\frac{\partial^2\theta_S}{\partial Y^2}\right)=0 \tag{6}$$

where $\mathrm{Re}=\frac{u_i L}{\upsilon}$, $\mathrm{Pr}=\frac{\upsilon}{\alpha}$, $Ha=B_0 L\sqrt{\frac{\sigma}{\mu}}$, $Ri=\frac{Gr}{\mathrm{Re}^2}$ are respectively the Reynolds number, Prandtl number, Hartmann number and Richardson number. $Q=qL^2/k_S\Delta T$ is the heat generating parameter, $K=\frac{k_s}{k}$ is the solid fluid thermal conductivity ratio.

Boundary Conditions: The dimensionless boundary conditions that are used in the present work can be set as follows:-

Inlet: $U=1, V=0, \theta=0$

Exit: convective boundary condition (CBC) $P=0$

At the bottom heated wall: $\theta=1$

At the left, right and top walls: $U=0, V=0, \frac{\partial\theta}{\partial N}=0$

At the solid-fluid interfaces: $\left(\frac{\partial\theta}{\partial N}\right)_{fluid}=K\left(\frac{\partial\theta_s}{\partial N}\right)_{solid}$

The average Nusselt number Nu_{av} at the hot wall is defined as $Nu_{av}=-\int_0^1\left(\frac{\partial\theta}{\partial Y}\right)dX$

and the bulk average fluid temperature in the cavity is defined as

$\theta_{av}=\int\theta\frac{d\overline{V}}{\overline{V}}$, where $\overline{V}$ is the volume of the enclosure.

The computational procedure is similar to the works performed by Ahammad et al. [4]. The governing nonlinear mass, momentum and energy equations are solved numerically by finite element method with Galerkin weighted residual scheme.

3 Model Validation Data

In order to test the validity of numerical code for the current study, a computation is carried out to compare with the numerical study of combined free and forced convection problem in a lid-driven enclosure having a circular body by Oztop et al. [9]. The relationships between the works of Oztop et al. [9] and present with good agreement in streamlines and isotherms are shown in Fig. 2. These validations make an affirmation of the current numerical code.

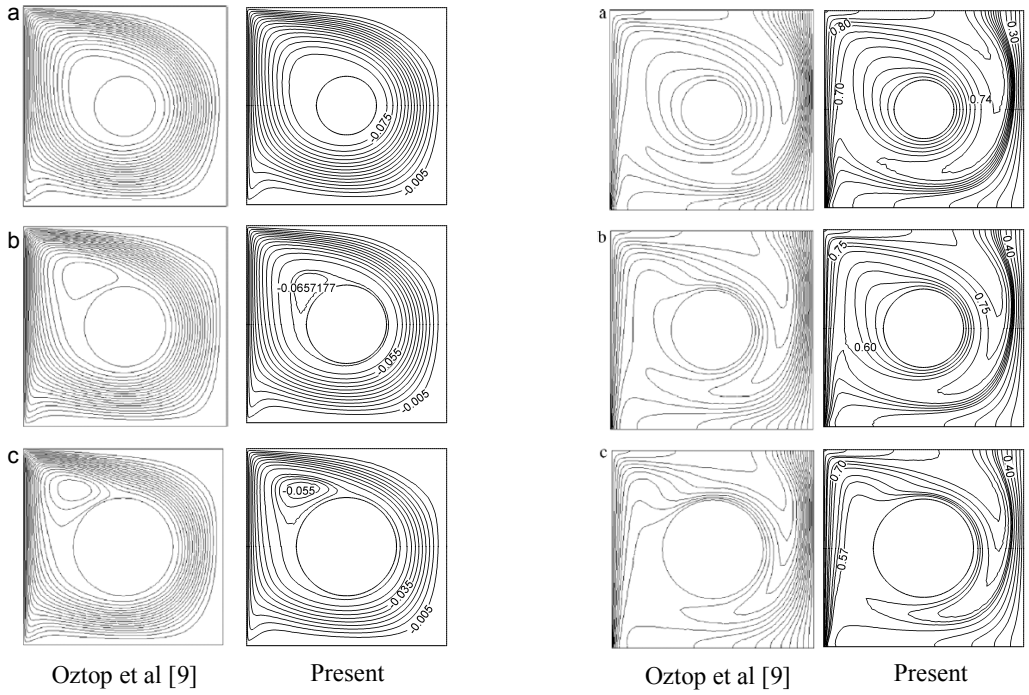

Fig. 2. Comparison of streamlines and isotherms for (a) $D = 0.3L$, (b) $D = 0.4L$ and (c) $D = 0.5L$ while $Gr = 10^5$, $Pr = 0.71$, $C = 0.5$ and $Re = 1000$

4 Results and Discussion

Fig. 3 depicts the streamlines and isotherms for three internal solid block with Reynolds number Re = 200 where Hartman number Ha and Prandtl number Pr are taken 10 and 0.71 respectively. The first column of Fig. 3(a) shows the streamlines for the heat generating body for three convective regimes of Richardson number Ri. When the dominant forced convection effect (Ri = 0.1) is considered, for the value of Re = 200 it is noticed that the fluid flow absorbs almost the whole cavity, diverges close to the heated surface and the open lines are symmetric about diagonally and a CCW vortex is created above the inflow openings. From this Fig. it can be highlighted that a noteworthy variation in flow behavior is found for the other two convective regimes of Ri (= 1, 10).

When Ri = 0.1, from the second column of Fig. 3(a) that represents the flow behavior for heat conducting obstacle it is seen that a unicellular vortex is created above the inlet opening and it expands very sharply for the higher values of Ri. in the last column of Fig. 3(a) flow patterns are presented for thermally isolated

body. A vortex is seen near the lower left side of the cavity, open lines shrinks towards the obstacle at Ri = 0.1 and this vortex enlarges very fast, consequently it captured the centered body as Ri increases.

The corresponding effect of inner blocks on the thermal field is exposed in the Fig. 3(*b*). In the case of heat generating body and all Ri (= 0.1, 1, 10), plume shape isotherms are viewed at the top side of the block. It also seen that thermal boundary-layer is created in the neighborhood of the bottom heated wall of the cavity and the isothermal lines become denser at the adjacent area of the heated block in the mixed convection and natural convection dominated regions.

The middle column exposes the temperature distribution for the case of heat conducting centered solid block. For the forced convection region Ri = 0.1, it is noticed that heat lines are nonlinear that stretched the whole cavity and a small variation is found for different values of Richardson numbers. Also the isotherms are packed at the inlet and form a boundary layer in the vicinity of bottom hot wall of the cavity. In the case of two upper values of Ri (= 1, 10), a tendency is observable for the low temperature heat lines is coming back towards the left wall of the enclosure.

In order to clearly exhibit the thermal field characteristic of the working area for the adiabatic obstacle the corresponding isotherms are displayed in third column of Fig. 3(*b*). In the dominant forced convection and pure mixed convection area it can be easily followed that isotherms are shrink gradually in the direction of bottom-right sided wall where as heatlines are found denser at the bottom surface in the case of Ri = 10 and some folding isotherms are returned to the left wall.

Fig. 4 depicts the streamlines and isotherms for three internal solid block with Prandtl number Pr = 1 where Reynolds number Re and Hartman number Ha are taken 100 and 10 respectively. From the first column of Fig. 4(*a*), it is seen that at Ri = 0.1 and 1, a small recirculation cell is formed near the left bottom corner above the inlet in the cavity. This indicates that the fluid flow of the enclosure has been affected by the inertia force. But it is observed that for the dominant natural convection (Ri = 10) region the flow structure is influenced much.

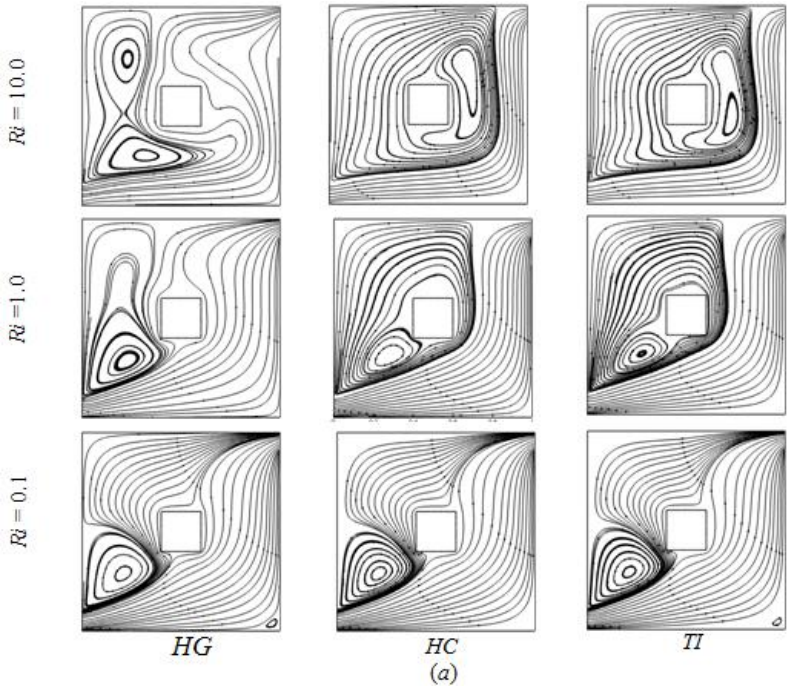

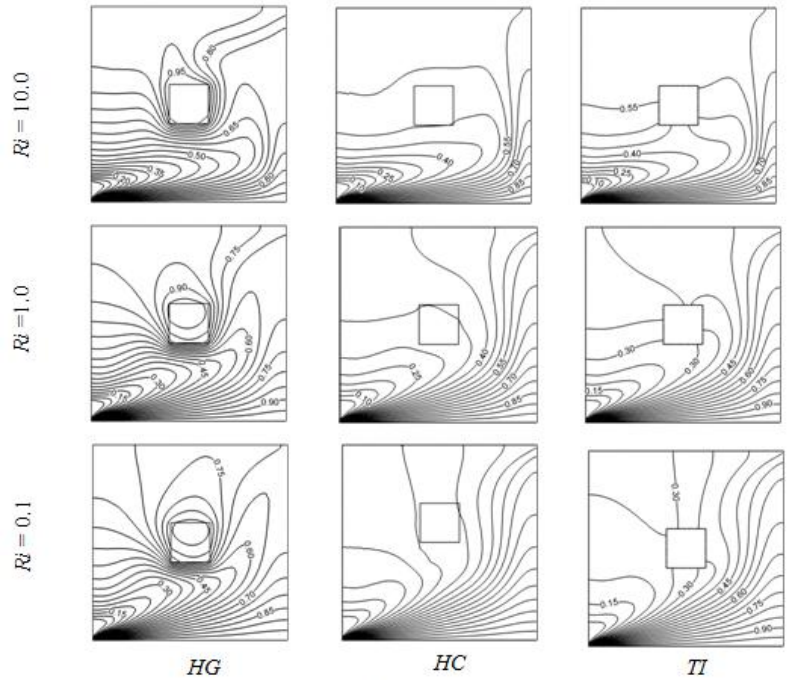

Fig. 3. (a) Streamlines and (b) isotherms for different values of *Ri*, with *Re*=200, *Ha*=10 and *Pr*=0.71

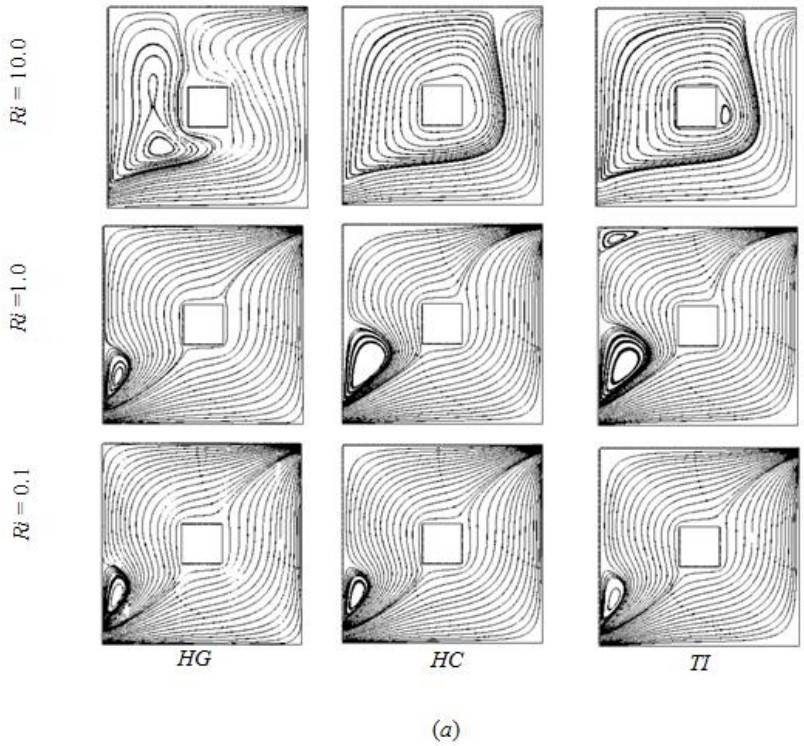

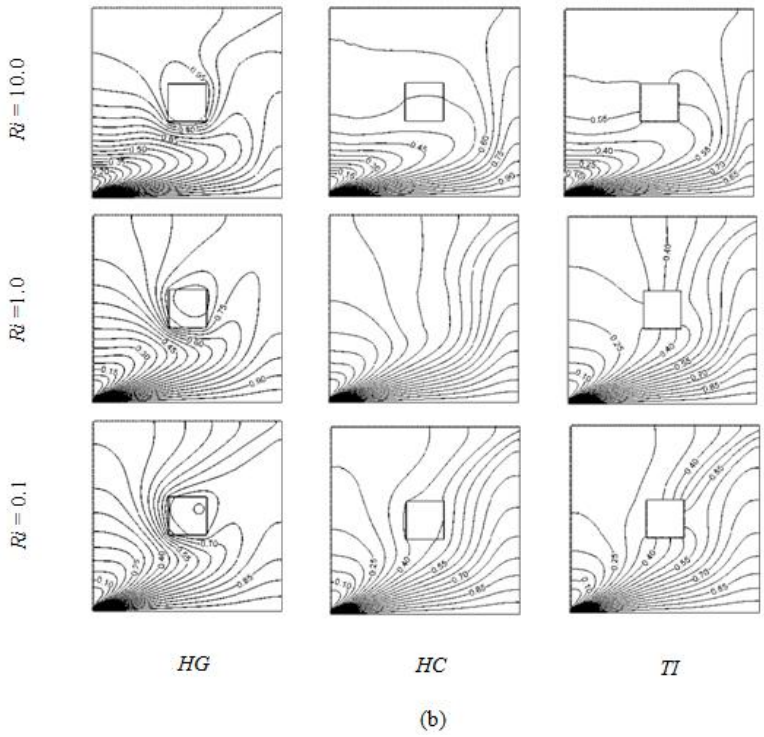

Fig. 4. (a) Streamlines and (b) isotherms for different values of *Ri*, with *Pr*=1, *Re*=100 and *Ha*=10

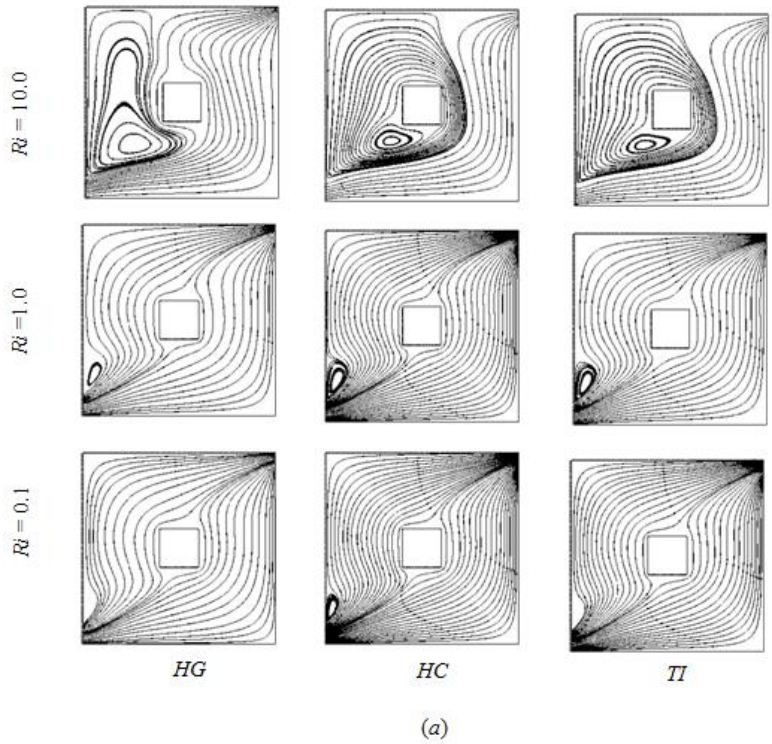

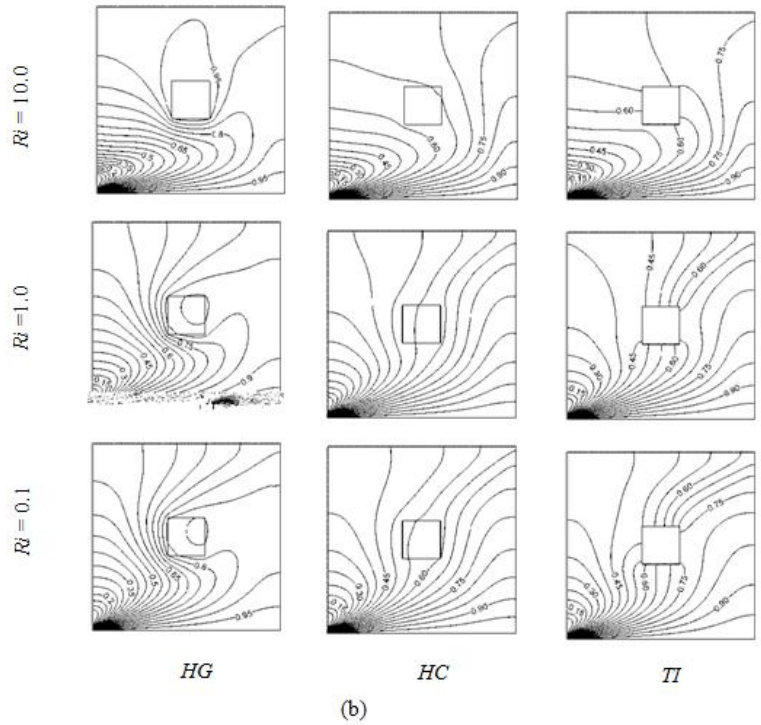

Fig. 5. (a) Streamlines and (b) isotherms for different values of *Ri*, with *Ha*=20, *Re*=100 and *Pr*=0.71

As the buoyancy force increases with increasing *Ri*; the rotating cell becomes larger for higher values of *Ri.*

The effect of heat conductive block placed at the center are presented in second column of Fig. 4(a). In the dominant forced convection region it is seen that a recirculation cell is formed just above the inflow opening and open lines are identical. At *Ri* = 1 the recirculation cell grows up. But when *Ri* = 10 a dramatically variation in flow patterns is noticed for the studied Prandtl number. Major streams minimize towards the right-bottom walls and consequently size of the vortex expands very swiftly and surrounded the inner block.

For the thermally isolated body that is shown in the third column of Fig. 4(*a*), it is found that in the dominant forced convection regime (*Ri* = 0.1) a small sized vortex is created above the inlet and open lines are stretched over the whole domain. When *Ri* = 1 the lower vortex enlarges and a small eddy is found at the left-top corner of the cavity. In dominant free convection regime (*Ri* = 10) the top row shows a noticeable change in flow characteristics. Size of the vortices increase very rapidly confining the centered body and thus main flow minimizes towards the bottom-right sides of the cavity.

Fig. 4(*b*) depicts the isotherms for the *HG*, *HC* and *TI* blocks with *Pr*=1. In the first column the figure illustrates that at *Ri* = 0.1 and *Ri* = 1 the heat lines become thinner and highest isotherm line pass through the heat generating block but at the dominant free convection region the isothermal line move out from the obstacle. It is seen that the isotherms become denser and top right cornered plume shape isotherms are created for *Ri* = 0.1, 1 whereas at *Ri* = 10, this type of heat lines are found at the top of the centered body.

For *Ri* = 0.1, 1, and 10 temperature distributions in middle column are followed almost the whole domain with thermal boundary layer at the bottom wall when *Pr* = 1.

In the case of adiabatic centered body, last column shows that the temperature distribution are found over the whole cavity for *Ri* = 0.1, 1 and for *Ri* = 10 heat lines are found to be reflected to the left wall.

The streamlines corresponding to studied three internal obstacles are shown in Fig. 5(*a*) where *Ha* =20 is considered and *Re* = 100, *Pr* = 0.71 is fixed. In dominant forced convection *Ri* = 0.1, from first column it can be noticed that the fluid flow is characterized by the open lines that squeezes above the inlet openings. When natural and forced convection are equally dominant, namely, *Ri* = 1, it is seen that the open lines swell up over the whole cavity and a small eddy is found above the inlet. For the convective regime *Ri* = 10, it is seen that the core vortex expands very sharply towards the right of the cavity and occupies the block indicating the enhancement of the flow strength of the vortex.

The effect of heat conductive block with Hartmann number are presented in second column of in Fig. 5(*a*). For the dominant forced convection area , at *Ha* = 20 it is followed that the fluid flow characterizes by the major streams through the cavity and a small vortex is found in the lower left side of the cavity. In the domain *Ri* = 1, flow patterns are almost identical and the vortex grows up. For the convective regime *Ri* = 10, at *Ha* = 20, the vortex shrinks from the right side and another vortex is seen below the obstacle.

Third column of Fig. 5(*a*) shows the influence of thermally isolated body and it is followed that an small rotating cell is created just above the inlet in the domain *Ri* = 1 whereas no vortex appears at *Ri* = 0.1. Interestingly, in the dominant free convection domain the patterns of the cavity flow change dramatically. The reality established here is that the application of transverse magnetic field acting as Lorentz's force which retards the flow.

Left column in Fig. 5(*b*), the corresponding isotherms for the aforementioned Hartmann number for the heat generating body is illustrated. In the regime of *Ri* = 0.1, the isothermal lines are crowded at the inlet and a thermal boundary layer is followed in the vicinity of the bottom hot wall of the cavity. Also a round shaped heat line appears through the square block. For *Ri* = 1, no significant change is found comparatively with that of the case at *Ri* = 0.1. Lastly for *Ri* = 10, it is noticed that the non-linearity of isotherms increases and the heat generating block is curbed by the topmost isothermal line.

The corresponding isotherms for the heat conductive block are displayed in second column of Fig. 5 (*b*). The heat lines are distributed through all over the cavity and isotherms are packed at the opening in the domain *Ri* = 0.1. Also a thermal boundary layer is formed in the vicinity of the bottom heated surface of the cavity. While *Ri* = 1, the isothermal lines are slight different. Lastly, in the dominant free convective regime *Ri* = 10, a markable change is observed.

The inspection of the heat lines profile relating to Hartmann number *Ha* = 20 are illustrated in right column of Fig. 5(*b*) for the case of thermally isolated body. The isothermal lines are scattered through all over the enclosure for the choosing value of Hartmann number in the different values of Richardson number regimes. However a noticeable variation is observed in the dominant natural convective domain at *Ha* = 20. Moreover, it is seen that heat lines are crowded at the bottom wall near the inlet port and a boundary layer is created at the vicinity of the heated surface of the cavity for each case.

Table 1. Average Nusselt number versus Richardson number for three different solid body with Reynolds number *Re* = 200

Ri	Nu_{av}		
	HG	***HC***	***TI***
0.1	7.750381	7.851059	7.839311
1.0	8.052749	8.326203	8.320327
10.0	9.454947	9.672471	9.671546

Average Nusselt number which is the representative of heat transfer at the bottom heated wall of the cavity containing different types of centered solid body separately with *Re* = 200 are tabulated in Table 1. Here considered three values of *Ri* is 0.1, 1, 10. From these values one can easily follows that in each case of Richardson number average Nusselt number Nu_{av} is maximum for *HC* block and minimum for *HG* block. Also free convection regime gives more heat transfer than forced convection and mixed convection regimes.

Table 2. Average Nusselt number versus Richardson number for three different solid body with Prandtl number *Pr* = 1

Ri	Nu_{av}		
	HG	***HC***	***TI***
0.1	6.401763	6.469222	6.46578
1.0	6.734086	6.861754	6.831039
10.0	7.580309	7.838668	7.827903

Table 2 shows the corresponding heat transfer at the bottom heated surface for the chosen three internal block with *Pr* = 1. From this table, it is observed that *HC* body gives optimum heat transfer whereas *HG* block gives lowest heat transfer.

Table 3. Average Nusselt number versus Richardson number for three different solid body with Hartman number *Ha* = 20.

Ri	Nu_{av}		
	HG	***HC***	***TI***
0.1	6.401763	6.469222	6.46578
1.0	6.734086	6.861754	6.831039
10.0	7.580309	7.838668	7.827903

Lastly, Table 3 presents the above mentioned values where *Ha* = 20 is taken and similar result is formed in this table also.

5 Conclusions

In this study, combined free and forced convective flows with thermal fields affected by the three different types of solid obstacle placed at the centre of the cavity with governing parameter *Re*, *Pr*, and *Ha* have been investigated. For a fixed value of Reynolds number *Re* = 200, it is found that heat conducting body gives the highest heat transfer at the bottom heated surface. On the other hand, lowest heat transfer from the heated wall is recorded for the case of heat generating block. A similar observation is followed for the other two parameters *Pr* = 1 and *Ha* = 20. Hence, it can be concluded that for all values of Richardson number R_i and *Re*, *Pr*, and *Ha* maximum cooling effectiveness can be achieved for the case of heat conducting block.

Competing Interests

Authors have declared that no competing interests exist.

References

[1] Rahman MM, Alim MA, Saha S, Chowdhury MK. Mixed convection in a vented square cavity with a heat conducting horizontal solid circular cylinder. Journal of Naval Architecture and Marine Engineering. 2008;5(2):37-46.

[2] Munshi MJH, Azad AK, Begum RA, Uddin MB, Rahman MM. Modeling and simulation of MHD convective heat transfer of channel flow having a cavity. International Journal of Mechanical and Materials Engineering. 2013;8(1):63-72.

[3] Prakash D, Ravikumar P. Study of thermal comfort in a room with windows at adjacent walls along with additional vents. Indian Journal of Science and Technology. 2013;6(6):4659-4669.

[4] Ahammad MU, Rahman MM, Rahman ML. Effect of inlet and outlet position in a ventilated cavity with a heat generating square block. Engineering e-Transaction. 2012;7(2):107–115.

[5] Rahman MM, Parvin S, Rahim NA, Islam MR, Saidur R, Hasanuzzaman M. Effects of Reynolds and Prandtl number on mixed convection in a ventilated cavity with a heat-generating solid circular block. Applied Mathematical Modeling. 2012;36:2056–2066.

[6] Loyola LT, Franco AT, Junqueira SLM, De Lai FC, Ganzarolli MM, Lage JL. Natural convection through an open cavity heated from the side and filled with fluid and discrete solid blocks. IMECE2013. Anais. In: ASME 2013 International Mechanical Engineering Congress & Exposition.

[7] Wanz Z, Yang M, Li L, Zhang Y. Combined heat transfer by natural convection – conduction and surface radiation in an open cavity under constant heat flux heating. Numerical Heat Transfer, Part A: Applications. 2011;60(4):289–304.

[8] Ait-Taleb T, Abedbaki A, Zrikem Z. Numerical simulation of coupled heat transfers by conduction, natural convection and radiation in hollow structures heated from below or above. International Journal of Thermal Sciences. 2008;47:378–387.

[9] Oztop HF, Zhao Z, Yu B. Fluid flow due to combined convection in lid-driven enclosure having a circular body. International Journal Heat and Fluid Flow. 2009;30:886–901.

[10] Rahaman MM, Billah MM, Saidur MAH, Hasanuzzaman M. Reynolds and Prandtl numbers effects on MHD mixed convection in a lid-driven cavity along with joule heating and centered heat conducting circular block. Int. Journal of Mechanical Materials Engineering. 2010;5(2):163-170.

[11] Ahammad MU, Rahman MM, Rahman ML. Mixed Convection Flow and Heat Transfer Behavior inside a Vented Enclosure in the Presence of Heat Generating Obstacle. International Journal of Innovation and Applied Studies. 2013;3(4):967-978.

[12] Gau C, Jeng YC, Liu CG. An experimental study on mixed convection in a horizontal rectangular channel heated from a side. ASME J. Heat Transfer. 2000;122:701-707.

[13] Kumar De A, Dalal A. A numerical study of natural convection around a square horizontal heated cylinder placed in an enclosure. International journal Heat Mass Transfer. 2006;49:4608-4623.

[14] Obayedullah M, Chowdhury MMK, Rahman MM. Natural convection in a rectangular cavity having internal energy sources and electrically conducting fluid with sinusoidal temperature at the bottom wall. International Journal of Mechanical and Materials Engineering. 2013;8(1):73-78.

[15] Rahman MM, Parvin S, Saidur R, Rahim NA. Magnetohydrodynamic mixed convection in a horizontal channel with an open cavity. International Communication Heat Mass Transfer. 2011;38: 184–193.

[16] Xu Xu, Yu Zitao, Hub Yacai, Fan Liwu, Cen Kefa. A numerical study of laminar natural convective heat transfer around a horizontal cylinder inside a concentric air-filled triangular enclosure. International Journal of Heat and Mass Transfer. 2010;53:345–355.

[17] Habibis S, Ammar IA, Ishak H. Natural convection in a differentially heated square enclosure with a solid polygon. Advances in Mechanical Engineering. 2015;7(12):1-10.

[18] Xu X, Yu Z, Hub Y, Fan L, Cen K. Transient natural convective heat transfer of a Low-Prandtl-Number fluid from a heated horizontal circular cylinder to its coaxial triangular enclosure. International Journal of Heat and Mass Transfer. 2012;55:995–1003.

[19] Calmidi VV, Mahajan RL. Mixed convection in a partially divided rectangular enclosure over a wide range of Reynolds and Grashof numbers. Int. J. Heat and Fluid Flow. 1998;19:358.

[20] Bhoite MT, Narasimham GSVL, Murthy MVK. Numerically the problem of mixed convection flow and heat transfer in a shallow enclosure with a series of block-like heat generating component for a range of Reynolds and Grashof numbers and block-to-fluid thermal conductivity ratios. International Journal of Thermodynamics and Science. 2005;44:125.
Available:http://dx.doi.org/10.1016/j.ijthermalsci.2004.07.003 11. 2005.

[21] Baranwal Ashok K. Chhabra Raj P. Effect of fluid yield stress on natural convection from horizontal cylinders in a square enclosure. Journal of Heat Transfer Engineering. 2016;38(6):557-577.
Available:http://dx.doi.org/10.1080/01457632.2016.1200373

[22] Shateyi Stanford. Heat and mass transfer for natural convection MHD flow over a permeable moving vertical plate with convective boundary condition in the presence of viscous dissipation. Frontiers in Heat and Mass Transfer (FHMT). 2017;9(7).
DOI: 10.5098/hmt.9.7

[23] Altaee Ali Hamza, Hassan Ali Farooq, Aadnan Mahdi Qusai. Natural convection inside square enclosure containing equilateral triangle with different orientations. Journal of Babylon University/Engineering Sciences. 2017;25(4).

[24] Ajaz Ahmad Dar Elangovan K. Thermal diffusion, radiation and inclined magnetic field effects on oscillatory flow in an asymmetric channel in presence of heat source and chemical reaction. Journal of Nigerian Mathematical Society. 2016;35(3):488-509.

[25] Abraham JP, Sparrow EM. A simple model and validating experiments for predicting the heat transfer to a load situated in an electrically heated oven. Journal of Food Engineering. 2004;62(4):409-415.

Peer-review history:
The peer review history for this paper can be accessed here (Please copy paste the total link in your browser address bar)
http://sciencedomain.org/review-history/22353